Proceedings of ERAD 2006

Brightband detection and evaluation using a radar simulator in a numerically-modelled atmospheric scenario

Luca Molini[1,2], A. Parodi[1,2], N. Rebora[1], F. S. Marzano[3], F. Siccardi[1,2]

[1] CIMA-Università di Genova, Savona (Italy).

[2] COS(OT), Industrial Consortium, Matera (Italy).

[3]DIE-Università La Sapienza, Rome (Italy).

1 Introduction

The use of weather radars is relevant for both precipitation rate retrieval and data assimilation purposes because of their capability to provide measurements of dynamical and microphysical states at high temporal and spatial resolutions. Nevertheless, a wide range of uncertainty sources affects radar measurement and its products, challenging their reliability. Radar simulation models have provided a suitable tool to investigate some of the main aspects of this issue since the early '90s: since here an exhausting treatment is not possible, we shall confine to cite the works of Chandrasekar and Bringi (1990), Krajewski and Anagnostou (1997), and Krajewski and Chandrasekar (1993). Haase and Crewell (2001) used the three dimensional fields of atmospheric variables generated by a numerical weather prediction model run at operative configuration (from 7 to 2.8 km horizontal grid spacing, see also Keil and Hagen, 2000; Meetschen and Crewell, 2000 and Pfeifer et al., 2004). This work focuses on the detection and quantification of the brightband effect on single polarised C-band radar measurements. The brightband effect is a typical electromagnetic phenomenon dealing with the melting processes of the solid hydrometeors occurring in the atmosphere. During the melting process, the hydrometeors are constituted by a mixture of ice, water and air and they show dimensions much larger than a corresponding liquid water drop. In this case, the electromagnetic response in terms of reflectivity is very enhanced producing a somewhat bright signature, since the name of "brightband".

Correspondence to: Luca Molini.

luca.m@cima.unige.it

this effect is characteristic of a stratiform pattern of precipitating structures since a less chaotic and turbulent dynamics can favour such a process. In terms of rain rate retrieval, if brightband-affected points are converted in precipitation, those intense echoes can lead to large overestimation of the rain field: detecting, recognizing and removing those artifacts is still an open issue. In order to deal with these uncertainty sources, Haase's approach is followed, while introducing some important enhancements we show in Section 4. First of all, a new brightband detection algorithm is implemented since in the original version of the radar simulation software we used the melting layer was modelled only by imposing atmospheric model is run at much higher resolution (1 km) in order to get closer to real radar spatial resolution. Then, coherently to a more precise dynamical modeling of the system, a more complete microphysical scheme is chosen so as to represent three precipitating species (rain, snow and graupel) instead of the two species used in the cited studies. A simplified atmospheric scenario is generated by the Lokal-Modell and standard radar products like plan position indicator (PPI) and range height indicator (RHI) scans are simulated by the radar simulator model. Simulations are performed either by considering uncertainty sources or not taking these factors into account so as to compare different datasets and determine an assessment of their influence on radar measurements. This study is organized as follows: Section 2 and 3 give a brief overview of Lokal-Modell and radar simulation model, Section 4 shows simulation results and quantitative analysis and finally, Section 5 contains conclusions and future outlooks.

2 The atmospheric model Lokal-Modell

The numerical simulations shown in this study are performed with the Lokal-Modell (LM) which is a non-hydrostatic and fully compressible numerical weather prediction model developed by Deutsche Wetterdienst (DWD, the German National Weather Service, Doms and Schättler, 1998). Such model uses hybrid terrain-following coordinates while the vertical resolution may be varied from a value of 50 m near surface up to several hundred metres according to altitude. The basic prognostic model variables are wind vector, temperature, pressure perturbation, specific humidity, rain water, cloud liquid water and cloud ice content while rain, snow and graupel fluxes are diagnostic variables. The Lokal-Modell offers a wide range of microphysical schemes spacing from the Kessler (warm rain) scheme to the 3-category ice scheme. For a more comprehensive description of the model, the reader is referred to Steppeler et al. (2003). In this study, the version 3.16 with a 3-category ice scheme is operated. The 3-category ice scheme allows the modeling of up to 6 microphysical species i.e. rain, snow, graupel, cloud water, cloud ice, water vapour and the related microphysical processes. The choice of such a complex microphysical scheme is mandatory due to the necessity of a reliable representation of the atmospheric processes at high resolution.

3 The Radar Simulator Model

The Radar Simulator Model (RSM) has been developed starting from Gunther Haase's master thesis (Haase, 2000) and it is able to simulate the most important atmospheric interactions of an electromagnetic wave with hydrometeors, e.g. backscattering and attenuation. In order to calculate the volume backscattering and extinction cross sections, some of the three-dimensional fields of an atmospheric model outputs (Lokal-Modell, in this case) are required: rain sedimentation flux, snow sedimentation flux, graupel sedimentation flux, temperature, pressure, cloud ice specific content, cloud water specific content and the water vapour ratio on which Mie scattering theory (Mie, 1908) is applied. so as to calculate either the volume absorption or scattering or backscattering cross section. The calculation of extinction cross section is performed by using the millimeter-wave propagation model of Liebe et al. (1989) which allows to consider the effects of absorption by atmospheric gases (e.g., molecular oxygen, water vapour and nitrogen). When all the contributions to radar response are computed, the backscattered power from the scanned volume to the radar can be expressed as follows:

$$\mathbf{P_r} = \mathbf{C_{rad}} \frac{1}{\mathbf{R}^4} \mathbf{V_p} \kappa_{\mathbf{back}} \, exp\left(-2 \int_0^{\mathbf{R}} \kappa_{\mathbf{ext}} \mathbf{dR} \right) \quad (1)$$

where C_{rad} is the radar constant (including the emitted power), k_{back} is a percentage of the whole scattered energy ($k_{back}=\alpha*k_{scat}$, $0<\alpha<1$), R is the range to the scattering volume and V_p is the pulse volume at range R. A relation between received power and reflectivity factor is determined by assuming only equivalent liquid particles (i.e. an equivalent radius is calculated both for snow and graupel) and pure Rayleigh scattering:

$$\mathbf{P_r} = \mathbf{C_{rad}} \frac{1}{\mathbf{R}^4} \mathbf{V_p} 10^{-10} \frac{\pi^5}{\lambda^4} |\mathbf{K}|^2 \mathbf{Z} \quad (2)$$

where $|K|^2 = 0.93$ is the dimensionless refraction constant for water. The combination of both equations (2) and (3) leads to the form below:

$$\mathbf{Z_{sim}} = 10^{10} \frac{\lambda^4}{\pi^5} \kappa_{\mathbf{back}} \, exp\left(-2 \int_0^{\mathbf{R}} \kappa_{\mathbf{ext}} \mathbf{dR} \right) \quad (3)$$

Usually, radar reflectivity is measured in dBZ = 10 log10(Z). RSM output consists of simulated PPI or RHI scans which actually consider radar beam geometry (and its effects on measurements). Moreover, RSM can calculate a reflectivity value for each domain grid point (reflectivity volume), just by summing up the contribution of each microphysical species without considering any physical interference to the measurement: in practice, the "true" reflectivity value for each grid point is provided.

4 The case study: 18 November 2004

During the night of 18 November 2004, a cold front arriving from outer Atlantic sectors reached Belgium, The Netherland and the northern part of Germany, causing a 48-hour event on these regions and a large amount of rain in the area covered by DWD radar network.

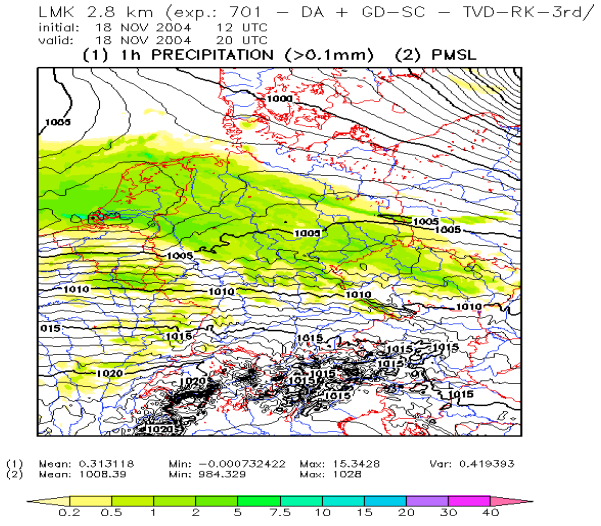

Fig. 1. The 18 Nov. 2004 event as forecast by 00.00 18-11-2004 run of the Lokal-Modell. A precipitation band over Germany an The Netherlands is clearly visible. *(courtesy of Thorsten Reinhardt, DWD, Offenbach)*

In order to reproduce the atmospheric conditions concerning this event, the Lokal-Modell is run in the official operational configuration with a 7-km horizontal grid spacing, 1.5 TKE closure, Tiedtke convective parameterization, 1-D turbulence scheme and 3-category ice scheme. The initial conditions are provided by the 00.00 GME model run of the 18-11-2004 as the hourly boundary conditions. Then, a nesting into 2.8-km horizontally resolved Lokal-Modell is performed by using the same setting except for the convective closure which is

here abandoned in favour of a explicit resolution of the convection. The next step consisted in comparing the original brightband (hereafter OLD_ALG) detection algorithm implemented in RSM and the new one (NEW_ALG) developed especially for this work. OLD_ALG is based essentially on a thermal threshold: i.e. if a solid hydrometeor finds itself crossing the 0°C isotherm, it is assumed to melt instantaneously and completely. To do that, from a modellistic point of view, the density and the dielectric constant of a snow (graupel) are replaced with the liquid water ones. NEW_ALG chooses the same brightband electromagnetic modelling, but it applies the procedure to the grid points for which a nonzero value of the melting rate is calculated by the atmospheric model. So as to quantify the differences between the algorithms, we select a vertical section of the domain volume for which the presence of melting solid hydrometeors is detected as it can be considered by the following figure.

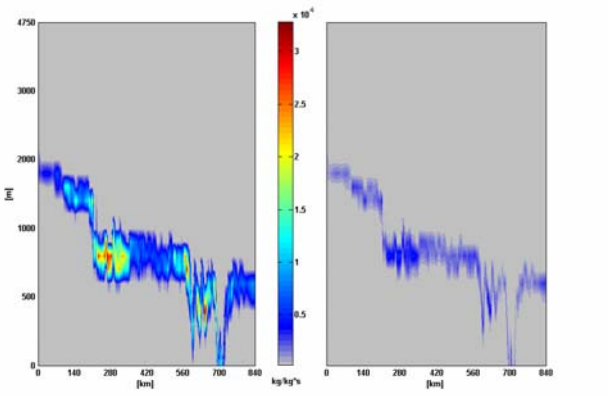

Fig. 2. The values of the melting rate calculated by the atmospheric model for a vertical section of the domain at 8 p.m: the sharp prevalence of snow production versus the graupel one (5 g/kg vs 0.7 g/kg, for the maxima, not shown), results in a larger melting rate.

Then, both algorithms are applied to the same vertical section by means of the RSM. The results are displayed in the following figure.

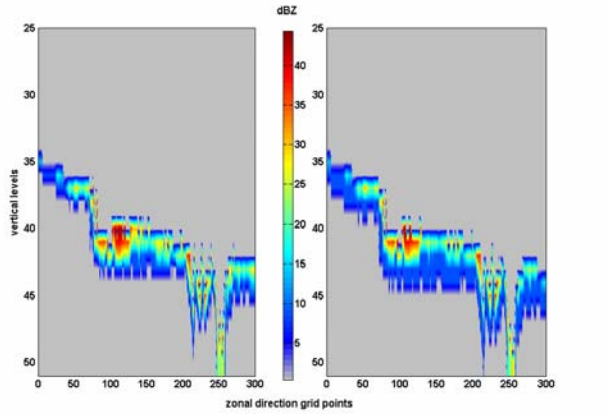

Fig. 3. The brightband detected with the OLD_ALG (on the left) and the NEW_ALG on the right, the representation seems to be quite similar even if a downward shift of the brightband can be noticed with the NEW_ALG.

Both algorithms are able to detect easily the presence of the brigthband: for clearness sake, only reflectivity due to melting particles is displayed. The differences between the methods can be highlighted by subtracting the OLD_ALG reflectivity dataset from the NEW_ALG one: in this way positive difference, calculated in dBZ, stand for points in which NEW_ALG outperform OLD_ALG.

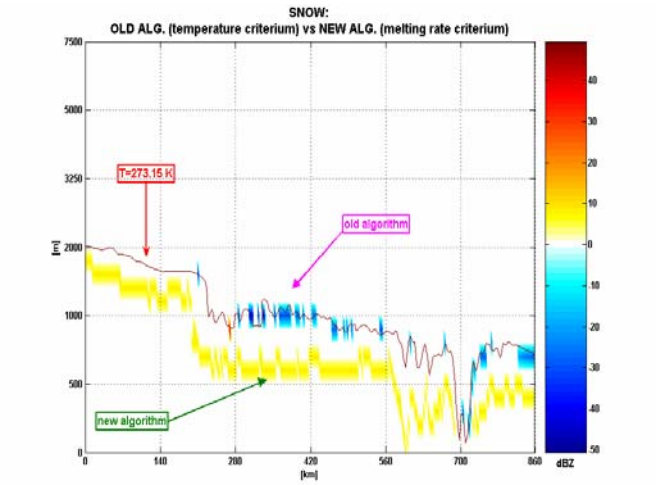

Fig. 4. The comparison between the different algorithms: the yellow layer points the re-location of the brightband due to the use of NEW_ALG.

As displayed in Fig. 4, by using NEW_ALG, the brightband is re-located up to 500 metres downwards, a non-negligible result if we wish to model in a better way the dynamical processes due to hydrometeors microphysics so as to perform a reliable radar measurement. From a statistic viewpoint, the number of the “melting grid points” of the domain calculated by each algorithm (see Fig. 5) is compared.

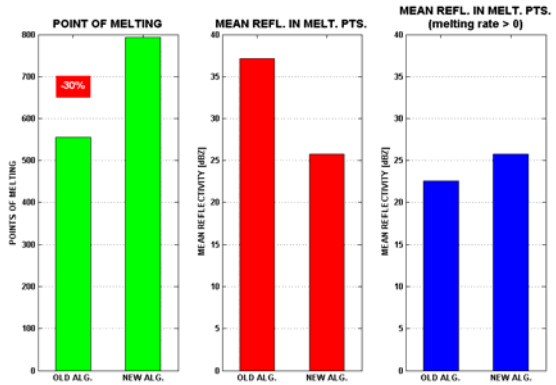

Fig. 5. Some statistics about the results retrieved using the two algorithm. NEW_ALG detects a major number of melting points (i.e. points in which a solid hydrometeors is melting, green bars) while the mean reflectivity of the brightband is minor respect of the one computed with OLD_ALG (red and blue bars).

The bars in Fig.5 show that NEW_ALG, using a microphysical threshold, can detect a number of melting points up to 30% more than OLD_ALG. On the other side, the mean reflectivity of the NEW_ALG-retrieved brightband is minor than OLD_ALG one, mainly in layers immediately below the 0°C isotherm: this means that in these points, the melting phenomenon is not really taking place but it is only an artefact of OLD_ALG. Once that NEW_ALG

has been validated and inserted in the RSM code Finally, the overestimation due to the brightband effect can be quantified by georeferring the RSM on the position of the Emden DWD C-Band radar and then performing simulated PPI scans by using NEW_ALG and without employing any, so as to calculate a reflectivity field depending only on the mixing ratios of the precipitating species and their sedimentation fluxes but not on their transition state.

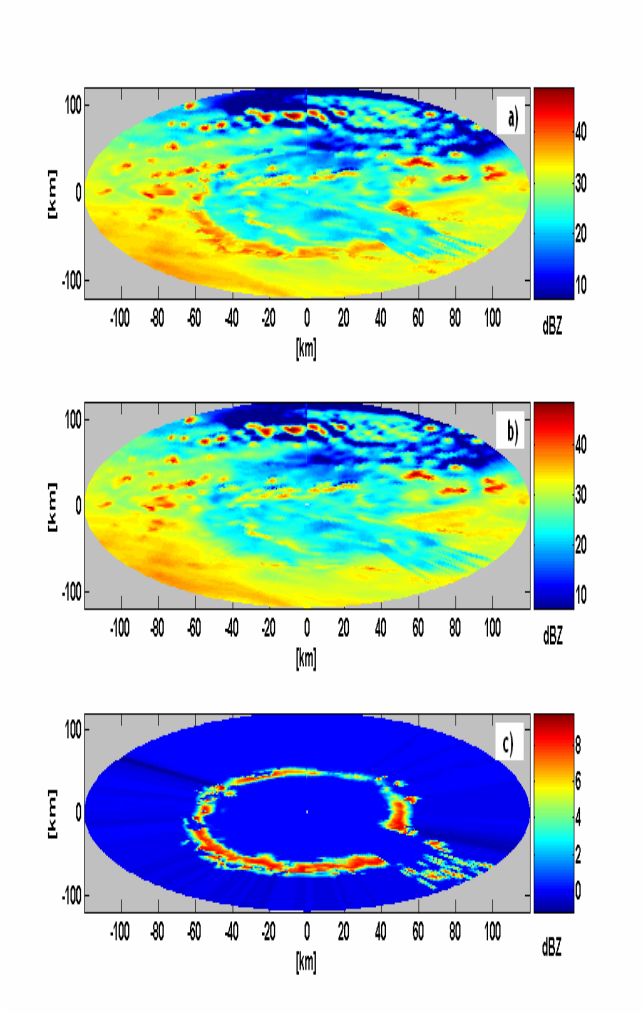

Fig. 6. Panel a) shows the PPI plot (performed at 0.5° elevation) obtained by applying NEW_ALG, panel b) the PPI with no brightband detection alghorithm, panel c) displays the between the two: the positive difference shows the overestimation due to the melting of solid hydrometeors.

By a simple comparison between the PPI scans, the brightband overestimation is very well evidenced as panel c displays the difference between the NEW_ALG PPI scan (panel a) and the same scan with no detection algorithms: the maxima are about 9 dBZ which means a deviation of several millimetres per hour if converted directly into rainrate at the ground.

5 Conclusions

A Lokal-Modell/Radar Simulator Model chain is used to test a new algorithm for brightband detection (NEW_ALG) implemented in RSM. This work shows some results about the use of this newly developed algorithm tested on the stratiform event occurred over North-Western Europe on 18 November 2004. NEW_ALG is able to reproduce the electromagnetic behaviour of melting hydrometeors in a good way by a dynamical and microphysical point of view by identifying as brightband points only grid points with a onzero melting rate . In particular, NEW_ALG can detect a major number of brightband points (by identifying as melting points the ones for which a nonzero melting rate is computed by the atmospheric model) respect to the old brightband detection algorithm (OLD_ALG) which uses only a thermal threshold. Moreover, the brightband is re-located by NEW_ALG some hundreds (up to 500) of metres downward, which means that even PPI scan performed with low elevation angles can be seriously affected by such a problem. Finally, just to give a brief example of how much brightband effect can spoil radar measurements, RSM has been georeferred on one of the DWD C-Band radars (sited in Emden, Lower Saxony, Germany) and PPI scans were performed from that position using a 0.5° degree elevation alternatively using NEW_ALG and not utilizing any brightband detection algorithms. The results show a mean overestimation due to melting processes of about 6 dBZ and maxima of about 9 dBZ: a large difference, which can lead to very bad performance of the system when converted into rainrate. Since by now, the melting rate variable has been used only as a binary brightband detector with no dependence on melting rate values, further work will be spent to calibrate NEW_ALG by finding a relationship between the melting index and the enhanced reflectivity signature and evaluating its performance on stratiform numerically modelled scenarios.

References

Chandrasekar, V., Bringi V.N.: Error Structure of Multiparameter radar And Surface Measurements of Rainfall Part III: Specific Differential Phase, *Journal of Atmospheric and Oceanographic Technology*, **7**,621-629,1990.

Doms, G., Schättler U.: The nonhydrostatic limited-area model LM (Lokal-Modell) of DWD, part I, Scientific Documentation, Offenbach, Germany, 1998.

Haase G., Crewell S.: Simulation of radar reflectivities using a mesoscale weather forecast model, *Water Resources Research*, **36**, 2221-2231, 2000.

Krajewski, W., Chandrasekar V.: Physically Based Radar Simulation of Radar Rainfall Data Using A Space Time Rainfall Model, *Journal of Applied Meteorology*, **32**, 268-283, 1993.

Krajewski, W., Anagnostou E.: Simulation of radar reflectivity fields: Algorithm formulation and evaluation, *Water Resources Research*, **33**, 1419-1428, 1997.

Meetschen, D., Crewell S.: Simulation of weather radar products from a mesoscale model, *Physical Chemistry Earth*, **25**, 1257-1261, 2000.

Steppeler, J., Hess, R., Doms, G., Schaettler, U. and Bonaventura, L: Review of numerical methods for non hydrostatic weather prediction models; *Meteorology and Atmospheric Physics*, **82**,287-301, 2003.